

# New frontiers in fractal boundary value problems

Alexander Teplyaev



University of Connecticut

CentraleSupélec  
Université Paris-Saclay



# Abstract:

Using non-smooth, or fractal, models in scientific and industrial applications is a very promising area of research, which may allow us to find optimal solutions to many problems not solvable by smooth methods. On the other hand, irregular or fractal objects and images are ubiquitous around us, from the smallest quantum scales to the structure of clusters of galaxies. Therefore, it is important in theory and in many applications to consider boundary value problems involving fractal domains. The talk will discuss the recent progress and challenges in adopting classical boundary value problems to the setting of non-smooth geometries. The potential applications include the better design of absorption materials, sharp recognition of non-smooth images, and faster algorithms for fluid dynamics computations. The presentation will be based on recent and in-progress joint work with Anna Rozanova-Pierrat, Frédéric Magoulès, Adrien Dekkers, Gabriel Claret (CentraleSupélec), Michael Hinz (Bielefeld), Luke Rogers (UConn), Maria Rosaria Lancia (Rome Sapienza), Patrick Ciarlet (ENSTA Paris).

# Plan of the talk:

1. Introduction and motivation
2. Wave absorption: numerical shape optimization
3. Wave absorption: theoretical shape optimization
4. Equations used in architecture
5. Wentzell Boundary conditions
  - 5.1 Theoretical study
  - 5.2 Discrete approximations
6. New Frontiers: Layer potentials
  - 6.1 Riemann-Hilbert and Poincare variational problems
  - 6.2 Hilbert transform
7. New Frontiers: Maxwell and other vector equations

# 1. Introduction and motivation

- ▶ *\*Strichartz: A fractafold, a space that is locally modeled on a specified fractal, is the fractal equivalent of a manifold.*
- ▶ *A “fractafold” is to a fractal what a manifold is to a Euclidean half-space.*

*This is a part of the broader program to develop probabilistic, spectral and vector analysis on singular spaces by carefully building approximations by graphs or manifolds.*

# What is the first well-known appearance of fractals in science?

In a sense, the simplest possible fractal appears in the famous Zeno's paradoxes: Zeno of Elea (c. 495 – c. 430 BC) "Achilles and the Tortoise"

1. Achilles runs to the tortoise's starting point while the tortoise walks forward.
2. Achilles advances to where the tortoise was at the end of Step 1 while the tortoise goes yet further.
3. Achilles advances to where the tortoise was at the end of Step 2 while the tortoise goes yet further.  
Etc.

Apparently, Achilles never overtakes the tortoise, since however many steps he completes, the tortoise remains ahead of him.

Dichotomy paradox: that which is in locomotion must arrive at the half-way stage before it arrives at the goal. In a race, the quickest runner can never overtake the slowest, since the pursuer must first reach the point whence the pursued started, so that the slower must always hold a lead. [Aristotle, Physics VI:9, 239b10, 239b15]

\*\*\*

In 1821, Augustin-Louis Cauchy proved that, for  $-1 < x < 1$ ,

$$a + ax + ax^2 + ax^3 + \dots = \frac{a}{1-x} := S(a, x)$$

This is a weakly-self-similar sum satisfying a re-normalization “fixed-point” functional equation

$$S(a, x) = a + x \cdot S(a, x)$$

# Cantor, Sierpinski, Julia, Mandelbrot

- ▶ How Long Is the Coast of Britain? Statistical Self-Similarity and Fractional Dimension (Mandelbrot 1967).

The coastline paradox: the measured length of a stretch of coastline depends on the scale of measurement.

Fractal titanium oxide under inverse 10-ns laser deposition in air and water. A. Pan, W. Wang, X. Mei, Q. Lin, J. Cui, K. Wang, Z. Zhai  
Applied Physics A volume 123, Article number: 253 (2017)

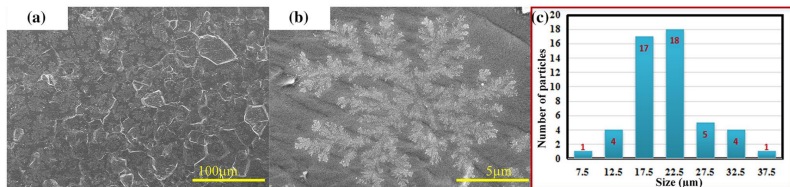


**Fig. 5** Surface morphology of titanium with the laser energy of 86 mJ, scanning speed of 0.01 mm/s, and scan length of 10 mm. *Inset a* depicts the surface morphology beyond laser irradiation zone. *Inset*

**b** shows a typical fractal structure unit, and *inset c* is size distribution histograms of 50 fractal structure units





## Superconducting disk with magnetic coating: Re-entrant Meissner phase, novel critical and vortex phenomena

M. V. MILOŠEVIĆ<sup>(a)</sup>, M. T. I. RAKIB and F. M. PEETERS<sup>(b)</sup>

*Departement Fysica, Universiteit Antwerpen - Groenenborgerlaan 171, B-2020 Antwerpen, Belgium*

received 28 September 2006; accepted in final form 22 November 2006

published online 22 January 2007

PACS **74.78.Na** – Mesoscopic and nanoscale systems

PACS **74.25.Op** – Mixed state, critical fields, and surface sheaths

**Abstract** – Within the Ginzburg-Landau formalism, we study the mixed state of a superconducting disk surrounded by a magnetic ring. The stray field of the magnet, concentrated at the rim of the superconducting disk, favors ring-like arrangement of induced vortices, to the point that even a *single vortex state exhibits asymmetry*. A novel route for the destruction of superconductivity with increasing magnetization of the magnetic coating is found: first all vortices leave the sample, and are replaced by a *re-entered Meissner phase* with a full depression of the order-parameter at the sample edge; subsequently, superconductivity is then gradually suppressed from the edge inwards, *contrary to the well-known surface superconductivity*. When exposed to an additional homogeneous magnetic field, we find a *field-polarity-dependent vortex structure* in our sample —for all vorticities, only giant- or multi-vortex states are found for given polarity of the external field. In large samples, the *number of vortex shells and number of flux quanta in each of them can be controlled* by the parameters of the magnetic coating.

Copyright © EPLA, 2007

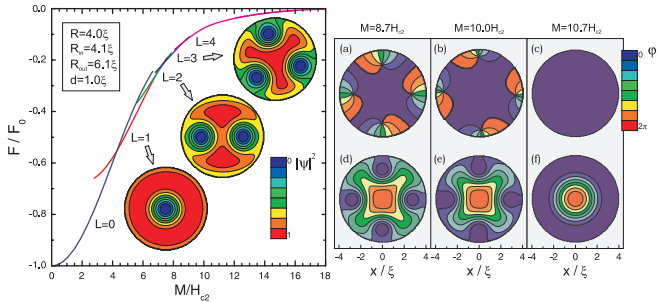


Fig. 2: The free energy of the states with different vorticity  $L$  as a function of the magnetization of the magnetic coating. Insets show the Cooper-pair density contourplots of the corresponding states. (a-c) Superconducting phase and (d-f)  $|\psi|^2$ -density plots, illustrate simultaneous vortex exit and suppression of superconductivity at the rim of the superconducting disk for high magnetization.

In our theoretical treatment of this system, we use the non-linear Ginzburg-Landau (GL) formalism, combined with Neumann boundary conditions (zero current penetrating the boundary). To investigate the superconducting state of a sample with volume  $V$ , we minimize, with respect to the order parameter  $\psi$ , the GL free energy

$$\mathcal{F} = \int \frac{dv}{V} \left( |(-i\vec{\nabla} - \vec{A}_H - \vec{A}_m)\psi|^2 - |\psi|^2 + \frac{1}{2}|\psi|^4 \right), \quad (2)$$

Minimization of eq. (2) leads to equations for the order parameter and superconducting current

$$(-i\vec{\nabla} - \vec{A})^2\psi = (1 - |\psi|^2)\psi, \quad (3)$$

$$\vec{j} = \Im(\psi^*\vec{\nabla}\psi) - |\psi|^2\vec{A}, \quad (4)$$

which we solve following a numerical approach proposed by Schweigert *et al.* (see ref. [2]) on a uniform Cartesian grid with typically 10 points/ $\xi$  in each direction. We then start from randomly generated initial distribution of  $\psi$ , increase/decrease the magnetization of the magnet or change the value of the applied external field, and let eq. (3) relax to its steady-state solution. In addition, we always recalculate the vortex structure starting from the pure Meissner state<sup>1</sup>( $\psi=1$ ) or the normal state ( $\psi\approx 0$ ) as initial condition. All stable states are then collected and their energies are compared to find the ground state configuration.

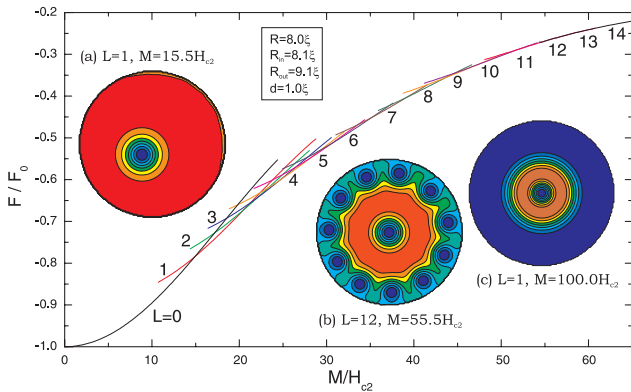


Fig. 3: Free energy diagram for a large superconducting disk with thin magnetic coating. Insets show the  $|\psi|^2$ -density plots of distinct vortex states.

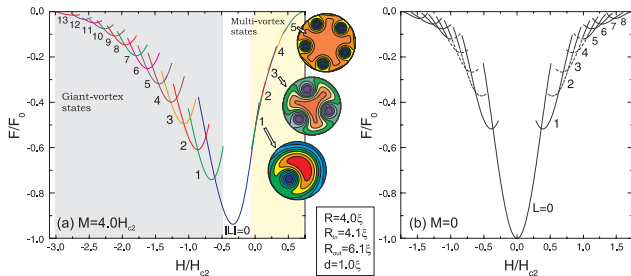


Fig. 4: (a) Free energy of a superconducting disk with magnetic coating as a function of applied homogeneous magnetic field. Insets show the Cooper-pair density plots for indicated states. (b) Same as (a), but for demagnetized coating. In (b), dashed lines denote multi-vortex and solid lines giant-vortex configurations.

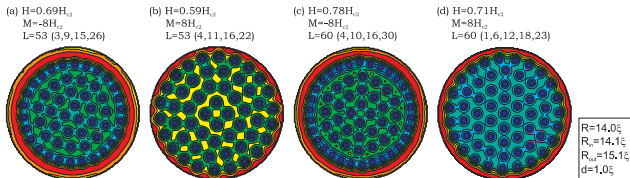


Fig. 5: The  $|\psi|^2$ -density plots illustrating the arrangement of vortex shells in a large superconducting disk for  $L=53$  and  $L=60$ , with magnetic coating with (a,c) negative ( $M=-8H_{c2}$ ), or (b,d) positive ( $M=8H_{c2}$ ) magnetization.

# GEOMETRICAL DESCRIPTION OF VORTICES IN GINZBURG-LANDAU BILLIARDS

E. AKKERMANS

Laboratoire de Physique des Solides  
and LPTMS, 91405 Orsay Cedex,  
France  
and

Physics Dept. Technion, Israel  
Institute of Technology, Haifa 32000,  
Israel



## 4.2 The Bogomol'nyi identities

For the special value  $\kappa = \frac{1}{\sqrt{2}}$ , the equations for  $\psi$  and  $\vec{A}$  can be reduced to first order differential equations. This special point was first used by Sarma [41] in his discussion of type-I *vs.* type-II superconductors and then identified by Bogomol'nyi [40] in the more general context of stability and integrability of classical solutions of some quantum field theories. This special point is also called a duality point. We first review some properties of the Ginzburg-Landau free energy at the duality point. We use the following identity true for two dimensional systems

$$|(\vec{\nabla} - i\vec{A})\psi|^2 = |\mathcal{D}\psi|^2 + \vec{\nabla} \times \vec{j} + B|\psi|^2 \quad (64)$$

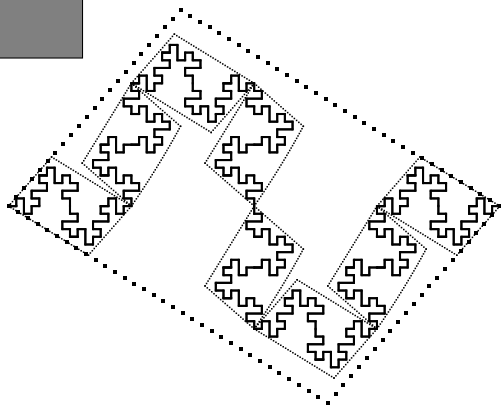
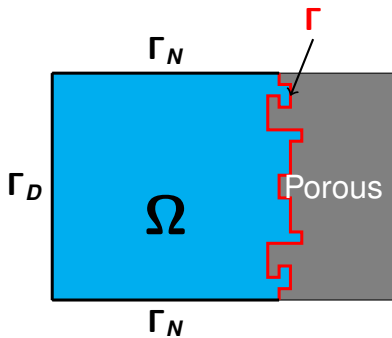
where  $\vec{j} = \text{Im}(\psi^* \vec{\nabla} \psi) - |\psi|^2 \vec{A}$  is the current density and the operator  $\mathcal{D}$  is defined as  $\mathcal{D} = \partial_x + i\partial_y - i(A_x + iA_y)$ . This relation is a relative of the Weitzenböck formula (61). At the duality point  $\kappa = \frac{1}{\sqrt{2}}$  the expression (63) for  $\mathcal{F}$  can be rewritten using (64) as

$$\mathcal{F} = \int_{\Omega} \left( \frac{1}{2} |B - 1 + |\psi|^2|^2 + |\mathcal{D}\psi|^2 \right) + \oint_{\partial\Omega} (\vec{j} + \vec{A}) \cdot \vec{dl} \quad (65)$$



## 2. Wave absorption: numerical shape optimization

- ▶ F. Magoulès, T.P. Kieu Nguyen, P. Omnes, A. Rozanova-Pierrat, Optimal absorption of acoustic waves by a boundary. SIAM J. Control Optimization 59 (2021)  
+ more numerical results
- ▶ C. Bardos, D. Grebenkov, A. Rozanova-Pierrat, Short-time heat diffusion in compact domains with discontinuous transmission boundary conditions. Math. Mod. Meth. Appl. Sci. 26 (2016)
- ▶ A. Rozanova-Pierrat, D. S. Grebenkov, and B. Sapoval, Faster diffusion across an irregular boundary. Phys. Rev. Lett. 108 (2012)



### 3. Wave absorption: theoretical shape optimization

- ▶ Anna Rozanova-Pierrat, "Generalization of Rellich–Kondrachov Theorem and Trace Compactness for Fractal Boundaries." Volume ICIAM 2019 Proceedings. Fractals in Engineering: Theoretical aspects and Numerical approximations. Springer International Publishing, 2021.
- ▶ A. Dekkers, A. Rozanova-Pierrat, Dirichlet boundary valued problems for linear and nonlinear wave equations on arbitrary and fractal domains, J. Math. Anal. Appl. 512 (2022)
- ▶ A. Dekkers, A. Rozanova-Pierrat, A. Teplyaev, Mixed boundary valued problems for linear and nonlinear wave equations in domains with fractal boundaries, Calc. Var. PDE 61 (2022)
- ▶ M. Hinz, A. Rozanova-Pierrat, A. Teplyaev Non-Lipschitz uniform domain shape optimization in linear acoustics SIAM J. Control Optim. 59 (2021)
- ▶ M. Hinz, A. Rozanova-Pierrat, A. Teplyaev Boundary value problems on non-Lipschitz uniform domains: Stability, compactness and the existence of optimal shapes Asymptotic Analysis (2023)

## 4. Equations used in architecture

- ▶ M. Hinz, F. Magoulès, A. Rozanova-Pierrat, M. Rynkovskaya, A. Teplyaev, On the existence of optimal shapes in architecture. Applied Mathematical Modelling 94 (2021)

Given a domain  $\Omega \subset \mathbb{R}^N$  and a vector field  $\mathbf{v} \in W^{1,2}(\Omega)^N$  we denote the symmetric part of its gradient by

$$\mathbf{e}(\mathbf{v}) = \frac{1}{2} (\nabla \mathbf{v} + (\nabla \mathbf{v})^t).$$

Let  $\mathbf{A} \in L^\infty(\Omega, \mathcal{M}_N^s(\alpha, \beta))$  and write  $\sigma(\mathbf{v}) = \mathbf{A}\mathbf{e}(\mathbf{v})$ ,  $\mathbf{v} \in W^{1,2}(\Omega)^N$ . We are interested in solutions  $\mathbf{u} \in W^{1,2}(\Omega)^N$  of BVP:

$$\begin{cases} -\operatorname{div} \sigma(\mathbf{u}) &= \mathbf{f} & \text{in } \Omega, \\ \mathbf{u} &= \mathbf{0} & \text{on } \Gamma_{\text{Dir}}, \\ \sigma(\mathbf{u}) \cdot \mathbf{n} &= \mathbf{g} & \text{on } \Gamma_{\text{Neu}}. \end{cases} \quad (1)$$

## 5. Wentzell Boundary conditions

- ▶ A. Wentzell. On boundary conditions for multi-dimensional diffusion processes. Theor. Probability Appl. (1959)

$$\mathcal{E}(u) = \int_{\Omega} \|\nabla u\|^2 dx + \mathcal{E}_{\partial\Omega}(u)$$

## 5.1 Theoretical study

- ▶ M. R. Lancia, P. Vernole,  
Venttsel' problems in fractal domains  
J. Evol. Equ. 14 (2014), no. 3, 681–712.

...

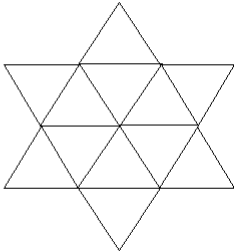
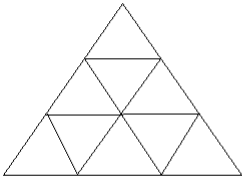
- ▶ M. Hinz, M. R. Lancia, A. Teplyaev, P. Vernole, Fractal snowflake domain diffusion with boundary and interior drifts, J. Math. Anal. Appl. 457 (2018)

$$\mathcal{E}(u) = \int_{\Omega} \|\nabla u\|^2 dx + \mathcal{E}_{\partial\Omega}(u)$$

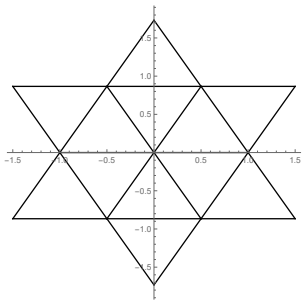
## 5.2 Discrete approximations

- ▶ M. Gabbard, C. Lima, G. Mograby, L. G. Rogers, A. Teplyaev, Discretization of the Koch Snowflake Domain with Boundary and Interior Energies, SEMA SIMAI Springer Series ICIAM2019 Fractals in engineering: Theoretical aspects and Numerical approximations (2021)

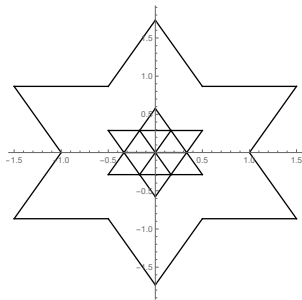
$$\mathcal{E}(u) = \int_{\Omega} \|\nabla u\|^2 dx + \mathcal{E}_{\partial\Omega}(u)$$



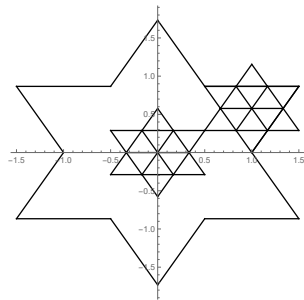




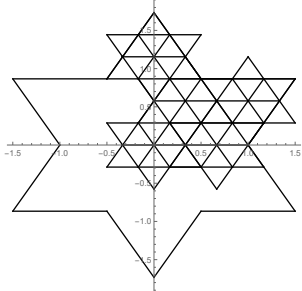
(a)



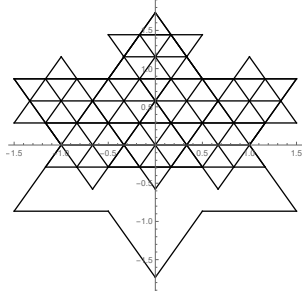
(b)



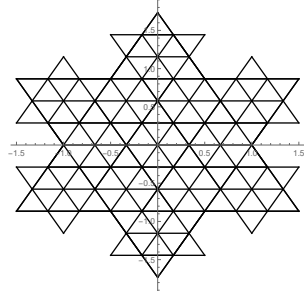
(c)



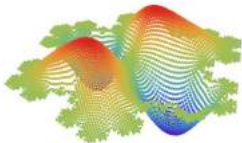
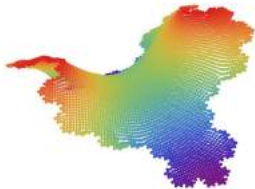
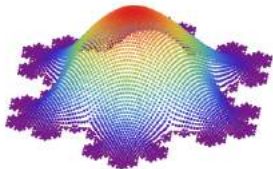
(d)

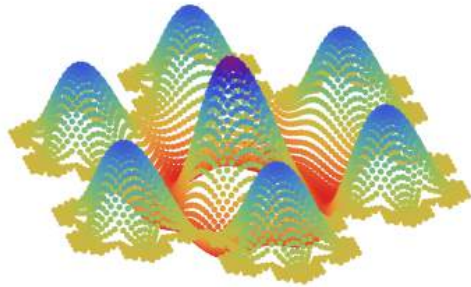
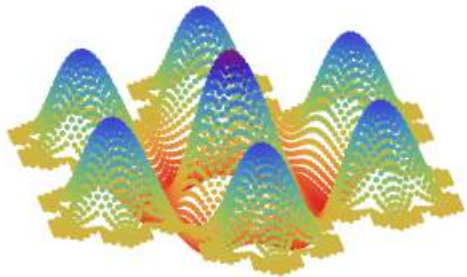


(e)



(f)





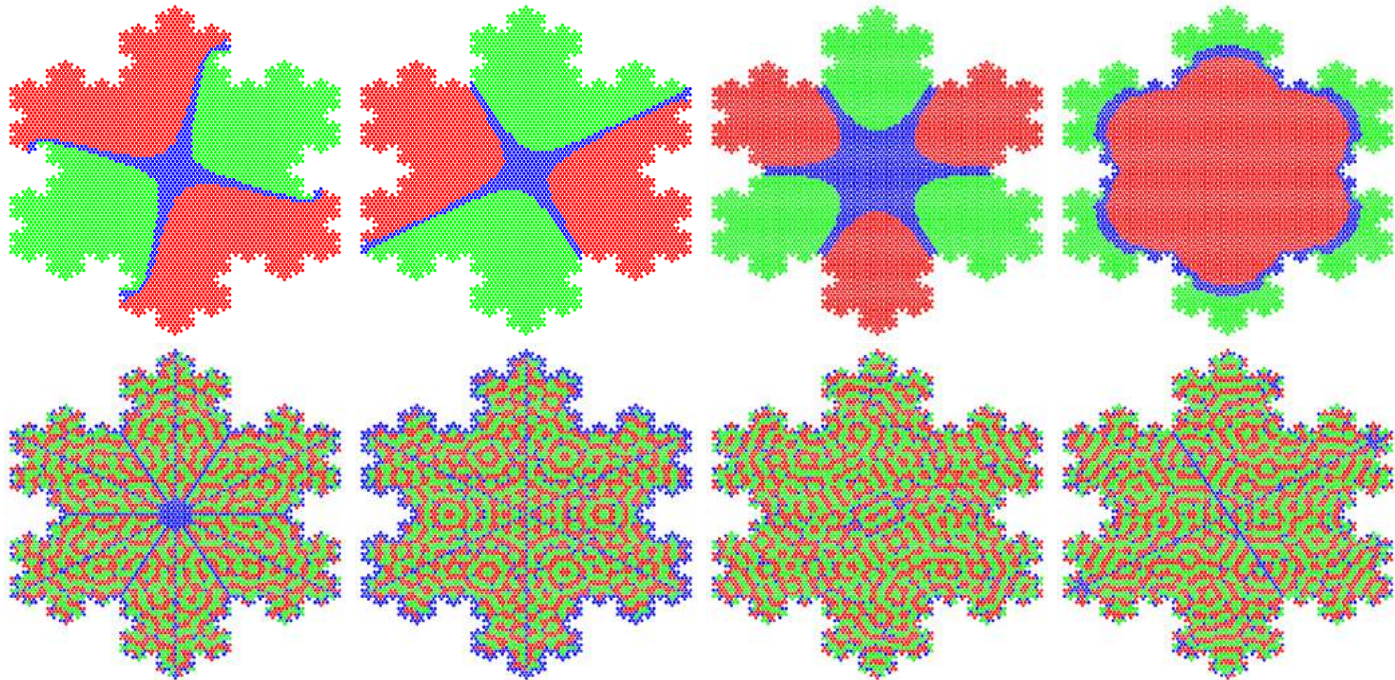


FIGURE 5. Contour Plots of the Eigenvectors of  $L_n$  corresponding to eigenvalues  $\lambda$ : (a) 4th eigenvector,  $\lambda = 48.1$ . (b) 5th eigenvector,  $\lambda = 48.1$ . (c) 6th eigenvector,  $\lambda = 85.1$ . (d) 8th eigenvector  $\lambda = 125.4$ . (e) 1153rd eigenvector  $\lambda = 49965.7$ . (f) 1157th eigenvector  $\lambda = 50156.6$ . (g) 1161st eigenvector,  $\lambda = 50188.8$  and (h) 1162nd eigenvector,  $\lambda = 50188.83$ . Blue regions indicate the values of an eigenvector in  $(-\epsilon, \epsilon)$ , red regions in  $(\epsilon, \infty)$  and green regions in  $(-\infty, -\epsilon)$ , where  $\epsilon = 0.01$ . (Level 4 graph approximation)

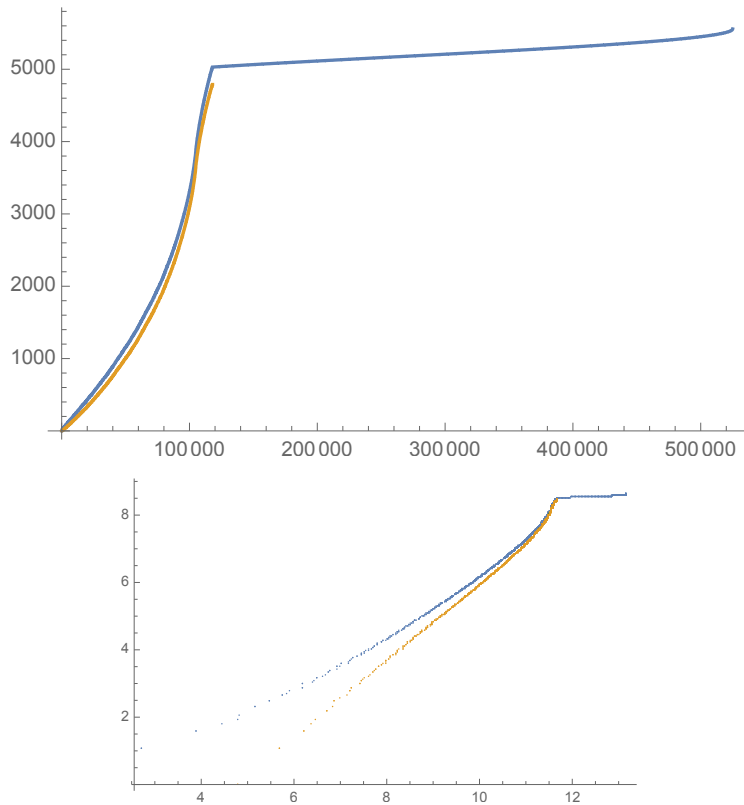


FIGURE 6. (Upper) Eigenvalue counting functions of Dirichlet Laplacian (orange) and  $L_n$  (blue). (Lower) Log-Log plot of the eigenvalue counting functions of Dirichlet Laplacian (orange) and  $L_n$  (blue) (Level 4 graph approximation).

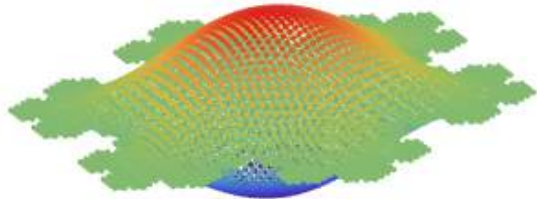


FIGURE 7. (a) The 5,028th eigenvector of  $L_n$ ,  $\lambda = 118038.02$ . (b) The last Dirichlet eigenvector,  $\lambda = 118039.37$ . The oval-shaped graph is due to a high oscillation of both eigenvectors

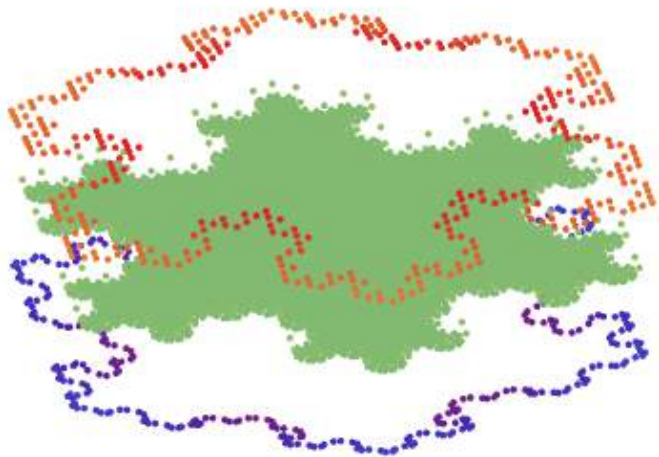


FIGURE 8. The last  $L_n$  eigenvector,  $\lambda = 524999.69$ . The graph splits into two parts, above and below the Koch snowflake domain due to a high oscillation (Level 4 graph approximation).



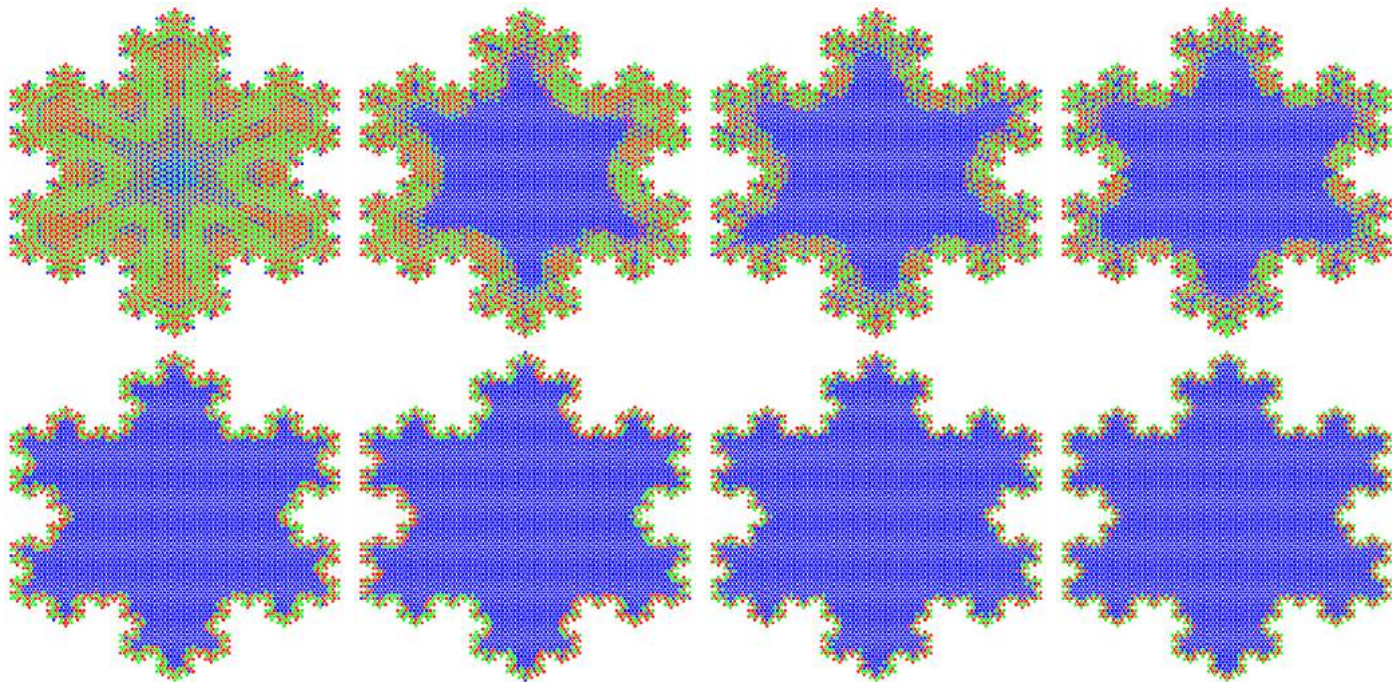
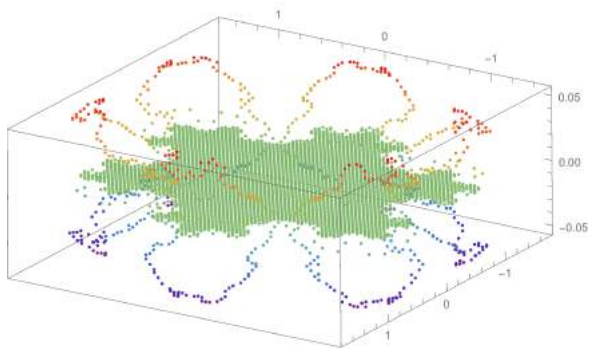
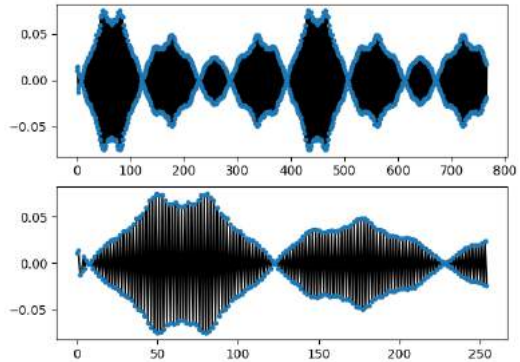


FIGURE 9.  $L_n$  eigenvectors localization with eigenvalues  $\lambda$ : (a) 5030th eigenvector,  $\lambda = 118048.66$ . (b) 5031th eigenvector,  $\lambda = 119678.65$ . (c) 5032th eigenvector,  $\lambda = 119678.65$ . (d) 5033th eigenvector,  $\lambda = 121460.72$ . (e) 5100th eigenvector,  $\lambda = 185367.41$ . (f) 5200th eigenvector,  $\lambda = 291364.38$ . (g) 5300th eigenvector,  $\lambda = 392584.97$ . (h) 5557th eigenvector,  $\lambda = 524999.69$ . Blue regions indicate the values of an eigenvector in  $(-\epsilon, \epsilon)$ , red regions in  $(\epsilon, \infty)$  and green regions in  $(-\infty, -\epsilon)$ , where  $\epsilon = 0.01$  (Level 4 graph approximation).



5550 Eigenvalue: 32945.826174



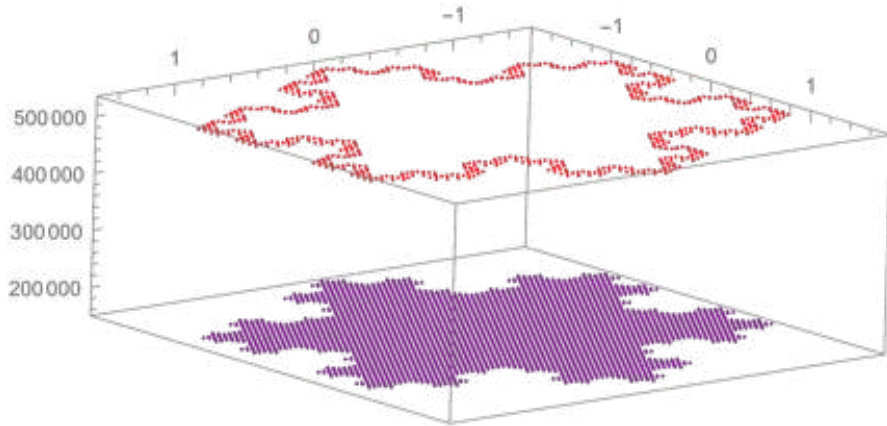


FIGURE 10. The high frequency landscape vector attains just the following two values the boundary vertices 527360 and 524288. It is constant on the interior vertices with the value 157464. (Level 4 graph approximation)

## 6. New Frontiers: Layer potentials

$$u(\mathbf{x}) = \int_S \rho(\mathbf{y}) \frac{\partial}{\partial \nu} P(\mathbf{x}, \mathbf{y}) d\sigma(\mathbf{y})$$

$$v(\mathbf{x}) = \mathbf{G} * \mathbf{f} = \int_{\mathbb{R}^n} \mathbf{g}(\mathbf{x}, \mathbf{y}) d\mu(\mathbf{y})$$

## 6.1 Riemann-Hilbert and Poincare variational problems

**Find a function in  $\mathbb{C}$ , unanalytic outside of a curve, with prescribed values and jumps on the curve.**

Research in progress: Anna Rozanova-Pierrat, Gabriel Claret (CentraleSupélec), Michael Hinz (Bielefeld).

Classical applications:

- ▶ Integrable models, inverse scattering or inverse spectral problem
- ▶ the inverse monodromy problem for Painlevé equations
- ▶ Orthogonal polynomials, Random matrices
- ▶ Combinatorial probability
- ▶ Algebraic geometry, Donaldson–Thomas theory

## 6.2 Hilbert transform

$$H(u)(t) = \frac{1}{\pi} p.v. \int_{\mathbb{R}} \frac{u(\tau)}{(t - \tau)} d\tau$$

Research in progress: Anna Rozanova-Pierrat, Gabriel Claret (CentraleSupélec), Michael Hinz (Bielefeld).

Closely connected to the Riemann-Hilbert and Poincaré variational problems and is extensively used in analysis and in signal processing.

## 7. New Frontiers: Maxwell and other vector equations

We develop new mathematical tools in the vector case in order to study and solve Maxwell's equations in non-Lipschitz, possibly fractal domains. To that extent, we would like to show here one use of those tools with the time-harmonic Maxwell problem completed with a homogeneous Dirichlet boundary condition, which becomes with our notations:

$$\begin{cases} \mathbf{curl}(\mu^{-1}\mathbf{curl} \mathbf{E}) - \omega^2\varepsilon\mathbf{E} = \mathbf{f} & \text{on } \Omega \\ \mathbf{Tr}_T(\mathbf{E}) = \mathbf{0} & \text{on } \partial\Omega \end{cases}$$

where  $\mathbf{f} \in \mathbf{L}^2(\Omega)$  and we look for  $\mathbf{E} \in \mathbf{H}(\mathbf{curl}, \Omega)$ .

This problem is equivalent to the following variational formulation:

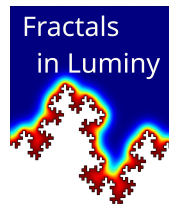
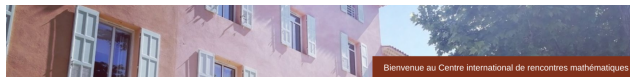
*Find  $\mathbf{E} \in \mathbf{H}_0(\mathbf{curl}, \Omega)$  such that  $\forall \mathbf{F} \in \mathbf{H}_0(\mathbf{curl}, \Omega)$ :*

$$(\mu^{-1}\mathbf{curl} \mathbf{E}, \mathbf{curl} \mathbf{F}) - \omega^2(\varepsilon\mathbf{E}, \mathbf{F}) = (\mathbf{f}, \mathbf{F}).$$

Research in progress: Anna Rozanova-Pierrat (CentraleSupélec), Patrick Ciarlet (ENSTA Paris) et al.

# Analysis on fractals and networks, and applications

18 – 22 March, 2024



Scientific Committee: Simon N. Chandler-Wilde (University of Reading), Marco Marletta (Cardiff University), Katarzyna Pietruska-Paluba (University of Warsaw), Alexander Teplyaev (University of Connecticut), Martina Zähle (Friedrich Schiller University Jena). Organizing Committee: Michael Hinz (Bielefeld University), Maria Rosaria Lancia (Sapienza University of Rome), Anna Rozanova-Pierrat (Université Paris-Saclay)

Thank you for your attention!